



How can the floor area types of a university campus mitigate the increase of urban air temperature?

Stefano Ponti¹ · Mauro Guglielmin¹

Received: 26 April 2022 / Revised: 13 January 2023 / Accepted: 14 March 2023
© The Author(s) 2023

Abstract

The urban heat island (UHI) under the current climate change scenario could have a major impact on the lives of urban residents. The presence of green areas undoubtedly mitigates the UHI, and modifies some selected anthropized surfaces with particular characteristics (e.g., albedo). Here, we use a university campus as a good template of the urban context to analyze the mitigation effect of different surface types on the air temperature warming. This study provides some of the best practices for the future management of land surface types in urban areas. Through the development of a simple air temperature mitigation index (ATMI) that uses the temperature, water content (WC), and albedo of the investigated surface types, we find the green and anthropized surfaces according to their areal distribution and mitigation effects. The findings address the importance of poorly managed green areas (few annual mowings) and anthropized materials that permit a good balance between water retention capacity and high albedo. In the case of impervious surfaces, priority should be given to light-colored materials with reduced pavement units (blocks or slabs) to reduce the UHI.

Keywords Urban heat island · Urban vegetation · University campus · Green management · Land surface type

Introduction

It is well known that the recent climate change has produced visible effects in the most sensitive areas (high altitude/latitude regions, (Masson-Delmotte et al. 2018)) with consequences on fragile ecosystems and landscapes, e.g., Ponti et al. (2021a). However, urbanized areas are also impacted by climate change particularly related to the increasing air temperature. Indeed, the urban heat island (UHI) effect is well known and, although mostly consistent with the near surface air temperature respect to the land surface temperature (Sun et al. 2020), it can increase the air temperature of urbanized areas (Cheval and Dumitrescu 2015). This increase is due to a series of consequences that follow a land-use change (Cetin 2020) such as: the urban canyon structures that reduce wind speed (Sen and Roesler 2017), the decrease of vegetation evapotranspiration (Thienelt and Anderson 2021), the increased impervious surfaces (Ziter et al. 2019) that prevent latent heat exchange (Miao and

Chen 2014), and decrease in albedo (Cotana et al. 2014). Furthermore, the heat stress effects on human health and well-being can increase human mortality (Rainham and Smoyer-Tomic 2003; Ragetti et al. 2017). Therefore, the adaptation/mitigation strategies are required not only for the services offered by urban ecosystems (Darrel Jenerette et al. 2011) but also for the well-being of the population (Klok and Kluck 2018; Zeren Cetin and Sevik 2020). Further, it is important to note that urban human activities can enhance the heat stress susceptibility (Knutson and Ploshay 2016), thus promoting positive feedback.

In urbanized environments, vegetation is one of the most studied surfaces that mitigates the UHI. Indeed, vegetation acts as a cooling island (CI) (Anniballe et al. 2014; Cetin 2015; Marando et al. 2019; Sebastiani et al. 2021) due to its shading (Picot 2004; Mariani et al. 2016) and the evapotranspiration from its surface, which reduce surface temperature (Mariani et al. 2016; Park et al. 2022). Moreover, the mitigation role of vegetation to climate change is twofold because it also inhibits the anthropogenic release of greenhouse gases while capturing and sequestering CO₂ (Shafique et al. 2020). Experiments have been conducted to understand which kind of management (Townsend-Small and Czimczik 2010; Gu et al. 2015) or plant species (Vaccari et al. 2013;

✉ Stefano Ponti
stefano.ponti@uninsubria.it

¹ Department of Theoretical and Applied Sciences, University of Insubria, Via J.H. Dunant, 3, 21100 Varese, Italy

Gratani et al. 2016) are the best choice for the carbon sequestration in urban contexts. Recently, studies focused on the mitigation effect of trees in urban areas (Zhou et al. 2017; Morakinyo et al. 2020; Rahman et al. 2020; Bozdogan Sert et al. 2021), but little research was conducted on the herbaceous component of lawns (Lee et al. 2016). Therefore, it is fundamental to know how to ameliorate urban herbaceous lawns to reach the potential of urban trees (Vaz Monteiro et al. 2016).

Recent research has highlighted the importance of UHI at a large scale (Kong et al. 2014; Kyriakodis and Santamouris 2018; Mirzaei et al. 2020), especially integrating remote sensing techniques with ground-based observations to spatialize the thermal stress over entire metropolises (Arghavani et al. 2020; Cao et al. 2021). However, the most utilized satellite sensors give an indication of the land surface temperature (LST) which is only the result of a surface energy balance (Takebayashi and Moriyama 2012). Therefore, recent advances in surface physical modeling might be an opportunity to fully explain the causes of UHI effects at a detailed or city-scale (Mariani et al. 2016; Marcel and Villot 2021).

Examples of UHI study in Italy are numerous, (e.g., Picot 2004; Anniballe et al. 2014; Mariani et al. 2016; Morini et al. 2018; Marando et al. 2019; Sebastiani et al. 2021), but they often focus on modeled effects and rarely show a collection of data in the field (Busato et al. 2014; Battista et al. 2020), that resemble both the green and anthropized surfaces (e.g., Battista et al. 2020). It is important to note that small-scale studies concerning the relationship between the land surface temperature and vegetation have focused on university campuses due to their similarity to small cities, (e.g., Srivanit and Hokao 2013; Addas et al. 2020) and their connection to the city socio-cultural economy (Cetin et al. 2021; Kalayci Onac et al. 2021). Indeed, university campuses represent small cities (Saadatian et al. 2013) with various land-use types (Wong et al. 2007). Within the urban environment, university campuses have an urban heat signature that cannot be excluded by the UHI analyses (Wibowo et al. 2019). If one considers that a number of universities have been investigated concerning their potential variation of UHI in metropolises (Lin et al. 2010; Xi et al. 2012; Geng et al. 2013; Feng et al. 2022) and that UHI affects also small towns (Borbora and Das 2014), then university campuses in small-size cities might have a crucial role.

In a framework of international university ranking of green campus and sustainability (Suwartha and Sari 2013), Italy adopted similar policies on the local territory in July 2015. The Italian University Network for Sustainable Development (RUS) (an apolitical coordination) was established to coordinate and share information about the environmental sustainability and social responsibility between all Italian universities. In this context, the main goal of RUS is

to spread the culture of sustainability by sharing skills and experiences within and outside Universities to increase the positive impact of environmental, ethical, social and economic actions, and to strengthen the recognizability and the value of the Italian experience on an international level (<https://reterus.it/en/goals-and-objectives/>). For this reason, the presented paper is necessary for the sharing of sustainable actions within the academic infrastructures as an example of correct management of the national territory. Therefore, the aims of this study are to: a) quantify the potential of different surface types to decrease the air temperature within the Insubria University campus (Italy), and b) list the mitigation properties for each material that need to be recommended for future choices (including costs).

Materials and methods

Study area

The study area is located at the western Insubria region from Lago di Varese to Lago di Como. It ranges from 45.75°N 8.85°E to 45.82°N 9.05°E. Insubria has long been recognized as a distinct bioclimatic region, characterized by its mild climate [35]. This area is characterized by a sub-continental climate, with a mean annual precipitation of 1600 mm, occurring in two main periods (April–May and October–November) and a mean annual temperature of 10–11 °C [36]. There is a negative W-E precipitation gradient that affects the seasonal pattern of precipitation with summer rains usually in the West (Lago Maggiore) and summer drought in the East [37].

The Insubria university area is divided into 3 zones/cities, each of which resembles several university campuses: Bizzozzero and Ravasi for Varese, Manara for Busto Arsizio and Valleggio, Abbondio, Natta, Cavallotti and Oriani for Como (Fig. 1). Varese has 79,800 inhabitants and a population density of 1450 inhabitants per square km, Como has 84,700 inhabitants and a population density of 2280 inhabitants per square km, and Busto Arsizio has 84,000 inhabitants and a population density of 2700 inhabitants per square km.

Weather and data collection

To describe the weather conditions of the sites for all 2020, 3 automatic weather stations (AWSs) were selected to be the closest to the three cities. The three AWSs' data were downloaded from the weather monitoring network of Lombardy Region (www.arpalombardia.it): (1) Busto Arsizio (45.6106°N, 8.8502°E, 222 m a.s.l.), (2) Varese (45.8325°N, 8.8236°E, 416 m a.s.l.), and (3) Como (45.8155°N, 9.0672°E, 201 m a.s.l.). The 3 AWSs were selected also to represent different urban settings in their neighborhood:

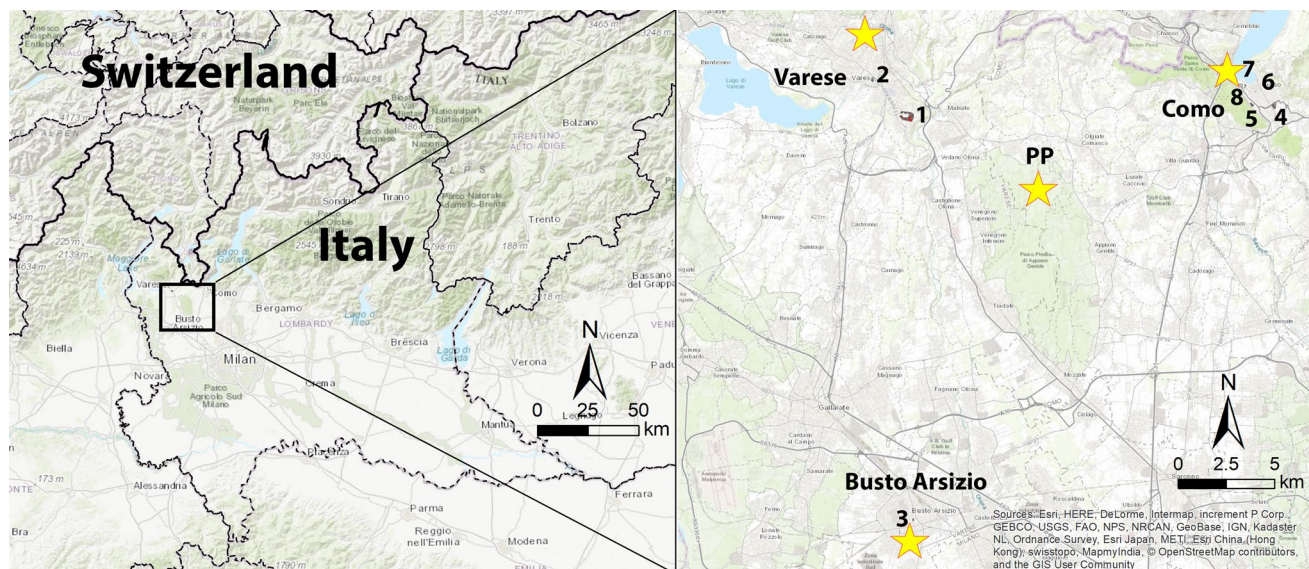


Fig. 1 The study area located in Northern Italy. The 2 yellow stars indicate the AWSs and the numbers the University detachments: 1=Bizzozzero, 2=Ravasi, 3=Manara, 4=Valleggio, 5=Abbon-

dio, 6=Natta, 7=Cavallotti, 8=Oriani. PP refers to the Parco Pineta automatic weather station (AWS)

more anthropized surfaces than green for Busto Arsizio, and half green and half anthropized for Como and Varese. In addition, a fourth AWS (Parco Pineta, PP) was chosen to represent the temperature difference between ground (at 10 cm of depth, under an herbaceous vegetated surface) and air (Centro Geofisico Prealpino, <https://www.astrogeo.va.it/meteo/>). The daily temperature differences were averaged with Varese AWS (which lays on an herbaceous mat) to have a general understanding of the annual heat exchange of the whole area (Fig. 2).

The fieldwork period, at the end of summer 2020, spanned from 28/09/2020 to 11/10/2020. This period was representative of the annual minimum variation of heat transfer between the surface and the air. Indeed, the annual standard deviation of air–ground daily temperature differences corresponds to 2.37 °C, whereas, during this study period, it is only 1.02 °C (Fig. 2a). Conversely, during summer and winter, the heat transfer can be amplified (Zajch and Gough 2021), with the occurrence of summer heat waves, soil moisture deficit (Whan et al. 2015), and high frequency of extreme events (Christidis et al. 2015). Moreover, photosynthesis and evapotranspiration can be reduced in summer due to stomatal closure (Zeiger et al. 1987). At these latitudes during spring, the frequent precipitation (Isotta et al. 2014) produced by the latitudinal oscillation of the North Atlantic Polar Front (Pinna 1996) is the main source of ground moisture which could alter the cooling effect of the green surfaces. The plant species and mean vegetation height (cm) for each type of lawn have been observed and measured in situ to assess the differences among the lawn types.

The choice of the surface types was taken by considering all the outdoor floor areas of the University Campus. In this sense, buildings were excluded from the study because vertical walls do not receive as much solar radiation as flat surfaces and roofs are difficult to access. Moreover, cool roofs are usually considered for the energy saving of buildings and not for outdoor floor areas that directly affect the human perception of the UHI. In addition, trees that cover a smaller total surface (21.5%) than grass lawns (78.5%) (example taken from Dunant, that is the zone with the highest number of trees) were also excluded. Each surface type was monitored once at the same period of the day (between 11:00 and 15:00 local time) to guarantee the zenith angle of the sun, and therefore the warmest moment of the day. Moreover, since it was not possible to investigate all the surfaces at once, additional monitoring days were selected on the basis of complete clear sky, no wind and after at least 2 consecutive dry days, therefore avoiding the precipitation occurring between 02/10/2020 and 05/10/2020 (Fig. 2b). A total of 87 measurements were conducted to guarantee at least 3 replicates for each surface type.

Surface temperatures were recorded by taking 3 randomly distributed images per surface type with a thermal camera (FLIR E85, 384 × 288 pixels, 0.1 °C of resolution, 2.0 °C of accuracy), calibrated in situ (Shea and Jamieson 2011). The temperature minimum, maximum, and mean value were recorded for each image.

The material mean WC (%) was recorded through 3 randomly distributed measurements per surface using a handheld dielectric moisture meter (Voltcraft MF-100) with a



Fig. 2 Climatic data of the closest AWSs. **a)** 2020 daily mean air temperature (°C) and daily temperature difference between ground (10 cm of depth) and air; **b)** Cumulative daily precipitation (mm), daily temperature difference between ground (10 cm of depth) and

air, and daily mean air temperature representing the measurement period. Please note that before each measurement, at least 2 full days of complete sun and no significant precipitation occurred

resolution and an accuracy of 0.1%. This is an easy tool to assess the construction materials moisture (Eklund et al. 2013). It recorded the mean WC within a range of depth of 2–4 cm.

The albedo was calculated as the ratio of the reflected radiation of the incoming radiation on a surface with a portable pyranometer (DeltaOhm LP 9221 S2, spectral range of 450–950 nm, resolution of 0.1 W m^{-2} , accuracy of 1.0 W m^{-2}). It was oriented perpendicularly to the surface at 50 cm above the surface. It was first directed to the surface, then directed in the opposite direction, 3 randomly distributed times per surface type.

Cost of the materials/surfaces has been expressed as the range of costs found on a) the Prezziario regionale delle opere pubbliche—2021 (www.regione.lombardia.it), and b) Assoverde price list 2019–2021 (www.assoverde.it). They are comprehensive costs that include materials and/or the

maintenance costs. It should be noted that the costs (€) per square meter refer to the entire amount. In this study, since it is not possible to forecast the descending price auction of the contractor company, we preferred to use the whole amount while keeping in mind that the real costs must be lower.

Social data were not considered in this analysis because the age of the University's frequenters is not representative of the population of the 3 cities and, in turn, it would not resemble the real socio-economical habits of the citizens. However, the results will be the base for a future multidisciplinary research.

Data analysis

The data analysis aims to present the recorded data in a simple output that represent the potential of mitigation of each surface type. It is for this reason that, for UHI studies,

it is the surface heat budget that governs the temperature perception, not only the surface temperature itself, as demonstrated by Eq. 1 (Takebayashi and Moriyama 2009):

$$R_n = H + G + IE, \quad (1)$$

where R_n is the net radiation (W m^{-2}), H the sensible heat flux (W m^{-2}), G the conduction heat flux (W m^{-2}), and IE the latent heat flux (W m^{-2}). It has to be kept in mind that, at stable conditions (no wind, same material, constant ambient temperature), albedo is the discriminating characteristic of the absorption of shortwave radiation, surface temperature is the discriminating characteristic of H while surface moisture of IE (Takebayashi and Moriyama 2009). Due to this, we suggest to use these properties for the construction of a simplified model that resembles the capability of a surface to increase or decrease the near surface air temperature. Indeed, when a surface or pavement is light colored (high albedo), retains more water (high water content) and has a high emissivity (low surface temperature) is usually cooler than the others (Santamouris 2014). Therefore, we propose here an equation based on the three simple measurable parameters discriminating the different energy balance components (albedo, water content, and surface temperature) for the air temperature mitigation index (ATMI) of a surface:

$$\text{ATMI} = \text{WC} A T^{-1}, \quad (2)$$

where WC is the volumetric water content of the material (%), A is the albedo of the surface (ranging between 0 and 1), and T is the mean surface temperature ($^{\circ}\text{C}$). The formula can be unitless and represents the easiest and fastest way to assess the energy budget of a surface. Indeed, the parameters are easily measurable with portable instruments and no samples for laboratory tests (thermal conductivity, density, heat capacity) are needed. This method guarantees a quick assessment for spatialization analysis.

The single recorded data were inserted into the equation as spatial mean values and a standard deviation of each parameter was also provided. Moreover, the maximum ATMI of the surface types was calculated by substituting the mean surface temperature with the minimum surface temperature.

The precision and accuracy of the datasets would lay on the repeatability of the measurement and the instrumental error. However, even at stable atmospheric conditions, the positioning of the instrument could differ from one measure to the second and affect the final data. It is for this reason that the equipment used was either already chosen/calibrated in previous publications (Schnepfleitner et al. 2016; Ponti et al. 2021b), or tested in the field such as the portable pyranometer with a white paper of known albedo. Moreover, to reduce errors, the operator and his position with the instrument was kept constant for each

measure and only the average value was used for the ATMI calculation.

Since the surface temperature is a consequence of the surface energy balance, a generalized linear model (GLM) with a backward stepwise method was conducted to test which of the measured parameters (air temperature, albedo, air relative humidity, and material type) majorly affected the surface temperature. Moreover, a multiple analysis of variance (MANOVA) and a one-way ANOVA were run to highlight the variance differences of ATMI and the measured parameters for each material type. All the above-mentioned analyses were performed using the software STATISTICA[®].

The spatial analysis was conducted in ArcGIS 10.8 (ESRI, Inc., Redlands, CA, USA): each surface type was digitalized throughout the university zones to obtain their areal extension (m^2). This permitted us to calculate a weighted average of the ATMI per university area, taking the sum of the product of the weights (surface types areas) times the ATMI value correspondent to each surface type divided by the sum of the areas.

Results

Surface type mitigation

A total of 26 surface types were identified and analyzed. Among the natural surfaces, 6 categories of green surfaces were identified, not only depending on the type of management, but also on the floristic composition and average vegetation height. The list of species differs among the lawn types; however, some of them (the most abundant) are widespread (*Poa pratensis*, *Trifolium pratense*). The lawns that usually undergo frequent mowings had an average height lower (15 cm) than those that undergo rare mowings (40 cm) (Table 1).

Overall, the surface temperatures were always greater than the air temperature recorded at the reference AWS, demonstrating that a sensible heat transfer toward the atmosphere was occurring, as assumed, except for the shrub lawn. This latter showed a mean surface temperature equal to the air temperature due to the shadow effect of the canopy. The highest temperature difference was measured at the interlocking block pavement made of vibrocompressed concrete² (17.9°C) and at the holed interlocking pavement made of concrete and gravel as filling (17.6°C). Apart from the shrub lawn, the minimum temperature difference was recorded at the porphyry pavement made of pink porphyry small blocks (0.7°C) and at the 4-mowing lawns (1.4°C). The mean WC varied considerably among the materials with values between 33.8% (asphalt) and 97.3% (3-mowing lawn). Smaller variations were recorded at surface types with the same material but different

Table 1 Characteristics of the green surfaces in terms of floristic composition and average vegetation height between mowings

Green surface type	Floristic composition	Average height (cm)
3-mowing lawn	<i>Achillea millefolium</i> , <i>Dactylis glomerata</i> , <i>Phleum sp.</i> , <i>Plantago lanceolata</i> , <i>Poa pratensis</i> , <i>Ranunculus acris</i> , <i>Rumex acetosa</i> , <i>Trifolium pratense</i>	15
4-mowing lawn	<i>Achillea millefolium</i> , <i>Geranium pusillum</i> , <i>Hieracium sp.</i> , <i>Poa pratensis</i> , <i>Rumex acetosa</i> , <i>Trifolium pratense</i>	25
8-mowing lawn	<i>Oxalis acetosella</i> , <i>Poa pratensis</i> , <i>Potentilla reptans</i> , <i>Ranunculus bulbosus</i> , <i>Trifolium pratense</i> , <i>Viola riviniana</i>	40
Shrub lawn	<i>Agrostis stolonifera</i> , <i>Poa pratensis</i> , <i>Trifolium pratense</i> and ornamental shrubs	10 (lawn), 60 (shrubs)
Hedge1	<i>Jasminum polyanthum</i>	200
Hedge2	<i>Jasminum polyanthum</i>	170

structures or dimensions such as the vibrocompressed concrete that ranged between 57.0% (type 2) and 64.0% (type 3). Generally smaller variations were obtained for the albedo that showed a minimum of 0.14 for the asphalt and a maximum of 0.27 for the shrub lawn and the white fine gravel (Table 2).

Figure 3 illustrates an example among the different university examined areas. We selected this example because it is the largest examined area and because here, there is a prevalence of green areas in which the different managements led to great ATMI differences. Moreover, the distribution of the green areas is heterogeneous and respects the

Table 2 Thermo-physical characteristics of the investigated materials and comparison with the air temperature at the AWSs correspondent to the time of the measurement. ΔT refers to the difference between

surface and air temperatures, while the mean values also show the \pm standard deviations

Item	Surface type	AWS AirT (°C)	ΔT (°C)	Mean temperature (°C)	Mean WC (%)	Mean Albedo
Lawn	3-mowing lawn	19.1	6.2	25.3 \pm 0.6	97.3 \pm 4.6	0.22 \pm 0.02
Lawn	4-mowing lawn	19.1	1.4	20.5 \pm 2.1	90.0 \pm 7.1	0.22 \pm 0.03
Lawn	8-mowing lawn	19.1	13.4	32.5 \pm 0.8	86.0 \pm 6.0	0.20 \pm 0.01
Shrub lawn	Shrub lawn	22.4	-0.1	22.3 \pm 0.6	71.3 \pm 4.2	0.27 \pm 0.19
Hedge	Hedge1	22.4	1.9	24.3 \pm 1.5	66.3 \pm 23.1	0.20 \pm 0.02
Hedge	Hedge2	18.4	3.3	21.7 \pm 1.5	51.3 \pm 21.5	0.17 \pm 0.06
Asphalt path	Asphalt	18.4	13.6	32.0 \pm 1.4	33.8 \pm 1.9	0.14 \pm 0.01
Asphalt path	Pink asphalt	18.4	5.9	24.3 \pm 0.6	39.0 \pm 2.6	0.17 \pm 0.01
Slab pavement	Concrete1	19.8	5.5	25.3 \pm 1.5	64.3 \pm 5.1	0.25 \pm 0.02
Slab pavement	Concrete2	22.4	11.6	34.0 \pm 0.0	69.7 \pm 5.9	0.24 \pm 0.01
Holed interlocking pavement	Concrete and gravel	19.1	17.6	36.7 \pm 0.6	41.3 \pm 7.8	0.18 \pm 0.01
Dirt parking	Mixed gravel	18.4	2.6	21.0 \pm 1.7	68.0 \pm 27.8	0.16 \pm 0.01
Gravel path	Medium gravel	19.1	8.9	28.0 \pm 1.0	56.3 \pm 13.6	0.18 \pm 0.0
Gravel path	White fine gravel	19.1	6.9	26.0 \pm 0.0	53.3 \pm 10.4	0.27 \pm 0.01
Parking	Pink fine gravel	19.1	7.9	27.0 \pm 1.0	54.0 \pm 6.6	0.23 \pm 0.01
Dirt road	Dirt road	18.4	1.9	20.3 \pm 1.2	57.0 \pm 8.2	0.15 \pm 0.01
Granite pavement	Granite block	19.8	5.2	25.0 \pm 1.0	64.7 \pm 12.1	0.22 \pm 0.02
Pebble pavement	Pebble	22.4	8.3	30.7 \pm 0.6	58.0 \pm 5.3	0.21 \pm 0.01
Porphyry pavement	Pink porphyry small block	17.3	0.7	18.0 \pm 2.6	64.3 \pm 1.5	0.16 \pm 0.02
Porphyry pavement	Large porphyry block	22.4	6.6	29.0 \pm 4.4	62.0 \pm 7.2	0.20 \pm 0.02
Porphyry pavement	Small porphyry block	22.4	5.9	28.3 \pm 0.6	53.7 \pm 2.1	0.17 \pm 0.01
Interlocking block pavement	Vibrocompressed concrete1	22.4	7.6	30.0 \pm 1.0	61.7 \pm 2.9	0.19 \pm 0.01
Interlocking block pavement	Vibrocompressed concrete2	19.1	17.9	37.0 \pm 1.0	57.0 \pm 3.6	0.17 \pm 0.02
Interlocking block pavement	Vibrocompressed concrete3	18.4	1.9	20.3 \pm 2.1	64.0 \pm 3.6	0.20 \pm 0.02
Pink block pavement	Vibrocompressed pink concrete1	18.4	8.6	27.0 \pm 2.6	50.3 \pm 0.6	0.18 \pm 0.0
Pink block pavement	Vibrocompressed pink concrete2	18.4	5.9	24.3 \pm 1.5	62.7 \pm 1.5	0.20 \pm 0.01

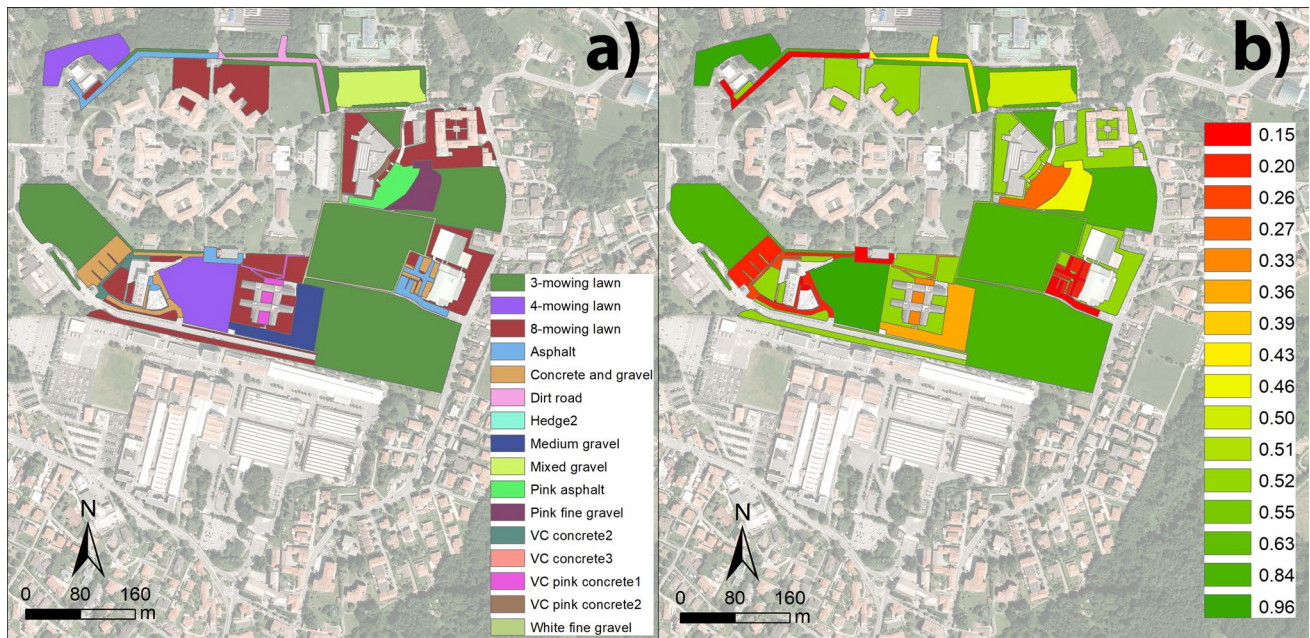


Fig. 3 The Bizzozzero University Campus: **a)** List of the surface types; **b)** their correspondent ATMI. VC = vibrocompressed

suggestions of Kong et al. (2014) for the mitigation property. Among them, the 4-mowing lawns are the best mitigating surfaces (ATMI 0.96), followed by other lawns in general (ATMI 0.52–0.84). The worst mitigating property is shown for asphalt paths (ATMI 0.15) and the holed interlocking pavement made of concrete and gravel (ATMI 0.20). The same trend of ATMI illustrated in Fig. 3b was found also at the other university areas.

The surface types also showed large differences of the ATMI in terms of means and ranges (Table 3). Among all, the 4-mowing lawn had the greatest mean ATMI (0.96), followed by the shrub lawn (0.86) and the 3-mowing lawn (0.84). Asphalt had the lowest mean ATMI (0.15), followed by concrete and gravel (0.20) and the pink asphalt (0.27). However, the range distribution did not perfectly match the mean ATMIs. Indeed, except for the 4-mowing lawn that had the largest range (0.87), the mixed gravel had the second largest range (0.59), followed by the 3-mowing lawn (0.51). The smallest ranges, instead, were recorded at the concrete and gravel (0.12) and the vibrocompressed concrete of type 1 and 2 (0.12). By grouping for the surface type category, the green areas had a mean ATMI of 0.69 and a mean ATMI range of 0.51, while the anthropized surfaces had a mean ATMI of 0.42 and a mean ATMI range of 0.24.

Within the green areas, the 4-mowing lawn was the best in terms of mean ATMI (0.96) and range (0.87), while hedge2 had the lowest mean ATMI (0.39) and the 8-mowing lawn the smallest range (0.31). Within the anthropized surfaces, concrete1 and vibrocompressed concrete3 had the highest ATMI (0.63), while asphalt (0.15) and concrete and

gravel (0.20) the lowest. The smallest range was recorded for the latter and the vibrocompressed concrete of type 1 and 2 (0.12) (Table 3).

The material surface temperature can be considered the result of the energy balance that is governed among all, not only by the material albedo and water content, but also by the air temperature and relative humidity (RH). The surface temperature, in turn, triggers a heat flux exchange able to increase or decrease the air temperature. It is for this reason that it is fundamental to understand what variable affects the material surface temperature. The GLM ($R^2 = 0.78$, $p < 0.001$) showed that the surface type is the only factor that statistically varies with the surface temperature variations ($F = 8.64$, $p < 0.001$) (Table 4). In a way, the surface type represents all of the material properties that drive the final surface temperature (even more than the external environmental conditions).

Since the surface temperature is driven by the interactions of the material properties (among which the albedo and WC), it is important to highlight the variability of the ATMI within the same materials (10 classes of surface types) to understand where interventions on the material characteristics are feasible to improve the ATMI. The MANOVA analysis showed a statistical difference among the 3 ATMI's components ($F = 5.69$, $p < 0.001$, 27 degrees of freedom). This demonstrates that the ATMI is amendable by acting on diverse measured properties, depending on the material type. Moreover, the one-way ANOVA showed that within the same component, there is a statistical difference of variance depending on the material type (Fig. 4).

Table 3 Mean ATMI of the investigated surface types and its range as maximum minus minimum ATMI calculated with maximum and minimum surface temperatures. The last column shows the average ATMI and range for all the green and anthropized areas

Item	Surface type	Mean ATMI	Max ATMI	ATMI Range	Mean ATMI/Range
Lawn	3-mowing lawn	0.84	1.01	0.51	0.69/0.51
Lawn	4-mowing lawn	0.96	1.40	0.87	
Lawn	8-mowing lawn	0.52	0.63	0.31	
Shrub lawn	Shrub lawn	0.86	1.02	0.41	0.42/0.24
Hedge	Hedge1	0.56	0.71	0.35	
Hedge	Hedge2	0.39	0.85	0.60	
Asphalt path	Asphalt	0.15	0.28	0.19	
Asphalt path	Pink asphalt	0.27	0.36	0.13	
Slab pavement	Concrete1	0.63	0.73	0.28	
Slab pavement	Concrete2	0.49	0.56	0.13	
Holed interlocking pavement	Concrete and gravel	0.20	0.28	0.12	
Dirt parking	Mixed gravel	0.50	0.88	0.59	
Gravel path	Medium gravel	0.36	0.56	0.27	
Gravel path	White fine gravel	0.55	0.65	0.23	
Parking	Pink fine gravel	0.46	0.56	0.19	
Dirt road	Dirt road	0.43	0.73	0.47	
Granite pavement	Granite block	0.57	0.65	0.14	
Pebble pavement	Pebble	0.40	0.53	0.24	
Porphyry pavement	Pink porphyry small block	0.56	0.77	0.32	
Porphyry pavement	Large porphyry block	0.43	0.54	0.21	
Porphyry pavement	Small porphyry block	0.33	0.41	0.18	
Interlocking block pavement	Vibrocompressed concrete1	0.39	0.44	0.12	
Interlocking block pavement	Vibrocompressed concrete2	0.26	0.34	0.12	
Interlocking block pavement	Vibrocompressed concrete3	0.63	0.85	0.43	
Pink block pavement	Vibrocompressed pink concrete1	0.33	0.47	0.21	
Pink block pavement	Vibrocompressed pink concrete2	0.51	0.69	0.28	

Table 4 Main factors affecting the mean surface temperature (dependent variable). The generalized linear model (GLM) was run on the 87 cases and with the surface type (26 classes) as categorical predictors

Factors	<i>F</i> value	<i>p</i>	<i>R</i> ²
RH	–	–	–
Albedo	–	–	–
Air temperature	–	–	–
Surface type	8.640	<0.001	
Full model	8.640	<0.001	0.78

The largest variability of ATMI was recorded for lawns (1.1), while the smallest for pebbles (0.07). Similarly, the largest variability of surface temperature was recorded for lawns (21.0 °C), while the smallest for pebbles (1.0 °C). Differently, hedges had the greatest WC variability (56%), while pebbles the lowest (10%). Again, lawns showed the greatest variability of albedo (0.34), while dirt road the smallest

(0.01) (Fig. 4). All the highest ATMI (favored) surface types per type of material are presented in Table 5.

Areal mitigation and costs

Among all of the university zones, the largest surface corresponds to the 3-mowing lawns (72,445.1 m²), followed by the 8-mowing lawns (44,162.5 m²), while the most restricted surfaces are hedge2 (151.5 m²) and pebbles (167.4 m²). The weighted average of the ATMI according to its areal extension is Valleggio the best mitigating university zone (0.69), followed by Bizzozzero (0.67). Conversely, the worst mitigating areas are Oriani (0.30) and Ravasi (0.42). Overall, the whole university area accounted for an ATMI of 0.66. Maintenance and posing costs of such surfaces vary between 0.15 (lawn mowing) and 97.21 € m⁻² (granite slab). However, for equal extension, it is important to note that surfaces with reduced maintenance costs could be more expensive than surfaces with cheaper posing costs, depending on the number of mowings or prunings. In this study, the total annual maintenance costs for the university green areas

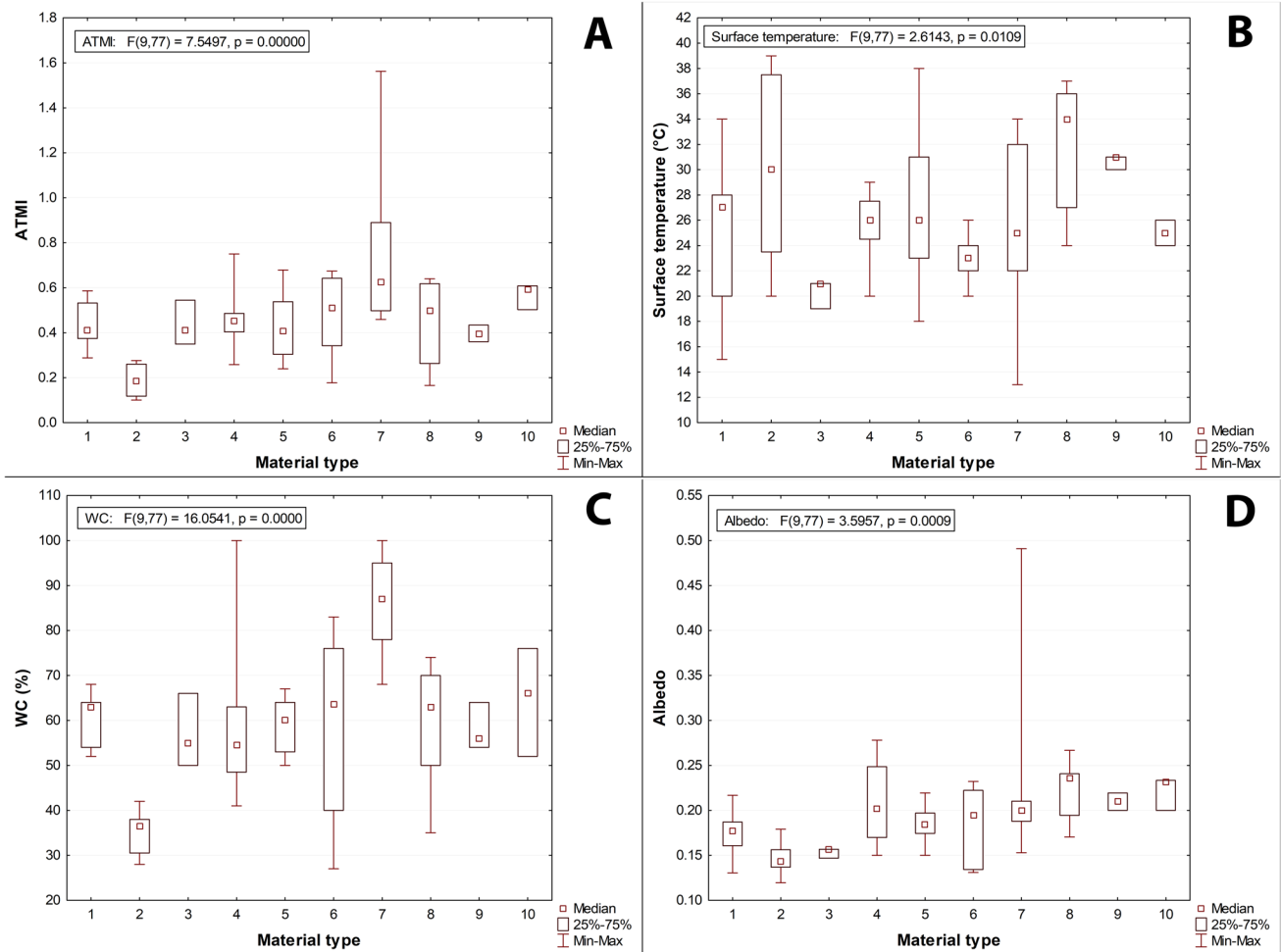


Fig. 4 Box and whisker plots that represent the median, minimum, maximum and quantiles of ATMI (a), surface temperature (b), WC (c), and albedo (d) per each material type (1–10, please see Table 5

for classification). At the top left of each panel, the summary of the one-way ANOVA analysis is shown

Table 5 Surface types classified according to their material (10 classes) and the most convenient action (I = increase, D = decrease) based on the variability of the material property (Temp = surface temperature). The last column indicates the best surface type per material that represents the action needed. - No choice of surface type within the material

Material	Figure 4 class	Action	Property	Favored surface type
Lawn	7	I	Albedo	3-mowing lawn
Hedge	6	I	WC	Hedge1
Asphalt	2	I	WC	Pink asphalt
Concrete	8	I	WC	Concrete2
Gravel	4	I	WC	Mixed gravel
Dirt road	3	I	WC	-
Granite	10	I	WC	-
Pebble	9	I	WC	-
Porphyry	1	D	Temp	Pink porphyry small block
Vibrocompressed concrete	5	D	Temp	Vibrocompressed concrete3

range between 69,060 and 82,250 €, while the total posing costs range between 2,897,426 and 3,616,984 €. This suggests that currently the active costs for only the maintenance of green areas are 2.3% of the posing costs sustained. Therefore, green areas will overcome the posing costs sustained with the current management in 50 years or more (Table 6).

Discussion

The methodology used in this study and the experimental design were kept easy, accessible, and rapid to facilitate urban planners or academic managers to either conduct cheap field surveys or to rely on easily accessible data, also collectable with other instrumentations.

The choice of the Insubria University campus well resembled the typical northern Italy territory, from green open spaces to urban environments with fragmented natural surfaces and totally anthropized areas. Indeed, the whole campus, spread in 3 cities with different urban contexts, gives an additional value to the general understanding of sustainability solutions in northern Italy.

The surface temperature of the investigated surface types showed large differences and, except for the shrub lawn, always higher than the air temperature at the time of the measurement. Indeed, the observed temperatures are the result of thermo-physical properties of the materials, such as albedo, emissivity, thermal conductivity, and permeability (Santamouris 2013). The material properties, assumed to be represented by the albedo and WC, are the major drivers of surface temperature at similar solar radiation input (Santamouris 2013; Taleghani 2018). Although the albedo did not considerably vary among the records (0.17–0.27), it is considered one of the largest controllers of air temperature mitigation (Zeren Cetin and Sevik 2020) and even CO₂ emissions (Akbari et al. 2009). It is difficult to define the primary variable that affected the surface temperature of the materials, even though it has been demonstrated that surface temperatures can be mainly attributed to the water content of the materials (Yamagata et al. 2008; Kinoshita et al. 2012). As a matter of fact, the latent heat flux related to the WC is able to decrease the surface temperature (Qin 2015) at similar atmospheric conditions (wind and RH). As a consequence, in this experiment, the variability of WC was the most common driver of the ATMI value. This is true for hedges, asphalts, concretes, gravel, dirt road, granite and pebbles.

It is difficult to find such simple surface properties collected in situ around the world. However, some authors who focused on the heat storage and the effect on the urban environment (Asaeda and Ca 1993, 2000; Asaeda et al. 1996) or the urban heat itself (Peña 2008), listed some surface properties that here we used to calculate the ATMI (Table 7) in

their study sites. It is, therefore, important to notice that in Japan and especially Tokyo, that has a similar climate to Northern Italy (Varese), has a lower minimum ATMI for soil (dirt road) and asphalt than our site. Conversely, looking at the vegetation ATMI, it is evident that Italy shows a much higher value than Chile and California, as well as for just soil (barren areas) in Chile. In this case, it is true that the climatic diversity among these locations affects the potential mitigation of the UHI (Debbage and Shepherd 2015). However, it should be kept in mind that the intensity of UHI might not be the same even at similar locations and climates (Mirzaei and Haghighat 2010), and therefore site-specific monitoring and mitigations are needed.

Green areas

For green areas like lawns that obviously had the highest WC, albedo was the variable with the greatest variation able to affect ATMI. Indeed, depending on the vegetation species, hairy shrubs on lawns considerably increased the albedo and, in turn, the ATMI. Similarly, taller herbaceous species (as consequence of less frequent mowings) had a higher albedo than shorter vegetation due to the quantity of green surface. For hedges, of which the WC had the largest variation, the canopy structure or the leaf area index (LAI) could have influenced the air humidity within the canopy (Hardwick et al. 2015), and thus could have affected the ATMI.

Other studies showed that the irrigation of anthropized surfaces highly mitigate extreme temperatures (Yamagata et al. 2008), especially if the WC is retained for a longer time (Nakayama and Fujita 2010). The fact that lawns showed such high WC values (71.3–97.3%) indicates not only the presence of moisture within the soil matrix but also within the organic matter tissues such as litter or roots that convey moisture to the surface and increase evaporation (Qin 2015). In a way, the presence of roots acts as a water reservoir so that the vegetated surfaces permit a twofold cooling process via evaporation of soil moisture and leaves' evapotranspiration (Tan et al. 2015).

For vegetated surfaces like lawns, the correct management is the reduction of annual mowings (Townsend-Small and Czimczik 2010; Gu et al. 2015) that increase the photosynthetic total surface, thereby augmenting evapotranspiration and ground shading (Tan et al. 2015; Mariani et al. 2016). Shading properties of vegetation against the UHI effect have been demonstrated (Tan et al. 2015, 2021; Park et al. 2022) and confirmed here in relation to taller vegetation. However, the fact that we recorded a higher ATMI for 4-mowing lawns than 3-mowing lawns is related to the difference of surface temperatures. At the time of measurement, the 3-mowing lawns underwent a mowing not being representative. Therefore, the vegetation height of the 3-mowing

Table 6 List of the surface type areas per each zone of the Insubria University with the maintenance/implementation costs per square meter and per year. The last row indicates the weighted average of ATMI according to the surface areas. * refers to the annual maintenance costs of green areas

Item	Surface type	Area (m ²)										Costs (€)		
		Total	Bizzozzero	Ravasi	Valleggio	Oriani	Abbondio	Cavallotti	Natta	Manara	Manara	Manara	€ m ⁻²	€ m ⁻² year ⁻¹
Lawn*	3-mowing lawn	72,445.1	68,397.8		143.3	22.5	3881.5						0.15–0.164	32,600–35,643
Lawn*	4-mowing lawn	18,829.3	13,291.2	516.8	5021.3								0.15–0.164	8473–9264
Lawn*	8-mowing lawn	44,162.5	31,472.1	1047.9	4629.2		3073	778	125.4	3036.9			0.16–0.164	19,873–21,727
Shrub lawn*	Shrub lawn	235.3					235.3						4.23–7.66	2985
Hedge*	Hedge1	398.1			73.8		193.1	131.2					3.11–7.66	3714–9148
Hedge*	Hedge2	151.5	127.1	24.4									3.11–7.66	1413–3481
Asphalt path	Asphalt	8860	5333.7	3526.3									10.0–11.8	265,799–313,642
Asphalt path	Pink asphalt	3007.9	3007.9										10.0–11.8	90,236–106,479
Slab pavement	Concrete1	3525.2			3525.2								28.92	305,845
Slab pavement	Concrete2	379.6			379.6								28.92	32,932
Holed interlocking pavement	Concrete and gravel	5663.6	5663.6										21.9–44.5	372,100–756,094
Dirt parking	Mixed gravel	6560.6	5975.3							585.2			5.3	104,312
Gravel path	Medium gravel	5531.4	5075.7								455.6		4.0	66,376
Gravel path	White fine gravel	1740.1	1740.1										4.0	20,880
Parking	Pink fine gravel	3167.7	3167.7										4.0	38,012
Dirt road	Dirt road	1762	1762										5.3	28,015
Granite pavement	Granite block	2641.2			2641.2								97.21	770,241
Pebble pavement	Pebble	167.4						167.4					51.02	25,622
Porphyry pavement	Pink porphyry small block	434.9		434.9									64.33–79.0	83,938–103,080
Porphyry pavement	Large porphyry block	317.2						317.2					88.2	83,925
Porphyry pavement	Small porphyry block	1743.8						1001.6		742.2			64.33–79.0	336,531–413,275
Interlocking block pavement	Vibrocompressed concrete1	762.1						762.1					22.81–37.5	52,148–85,732
Interlocking block pavement	Vibrocompressed concrete2	1013.4	743.2			270.2							22.81–37.5	69,349–114,012
Interlocking block pavement	Vibrocompressed concrete3	252	252										22.81–37.5	17,245–28,352
Pink block pavement	Vibrocompressed pink concrete1	1250.6	1250.6										22.81–37.5	85,580–140,696
Pink block pavement	Vibrocompressed pink concrete2	706.2	706.2										22.81–37.5	48,327–79,451
Weighted average		0.66	0.67	0.42	0.69	0.30	0.62	0.47	0.52	0.49	Total			2,966,486–3,699,235

Table 7 Comparison of ATMIs applied to different surface types at different locations in the world

Location	Surface type	Min ATMI	Mean ATMI	References
Northern Italy	Vegetation	0.45	0.77	This study
	Soil	0.26	0.43	
	Asphalt	0.10	0.15	
Mid Chile	Vegetation		0.23	Peña (2008)
	Soil		0.02	
	Asphalt			
Southern California	Vegetation		0.17	Sailor (1994)
	Soil			
	Asphalt			
Mid Japan	Vegetation			Asaeda and Ca (1993, 2000); Asaeda et al. (1996)
	Soil	0.11		
	Asphalt	0.07		

lawns produced less shadows, thus higher temperatures (Mariani et al. 2016). For hedges, it is recommended to choose non-compacted canopies, not only to increase the shading properties (Tan et al. 2015), but also to increase the air RH.

For our point of view, to extend the correct practices in urban contexts, it is necessary to not only rely on the good appearance of the green areas, neither on total abandonment, but rather a compromise of a functional vegetation-soil system (high shading, LAI, water retention) that needs little annual management.

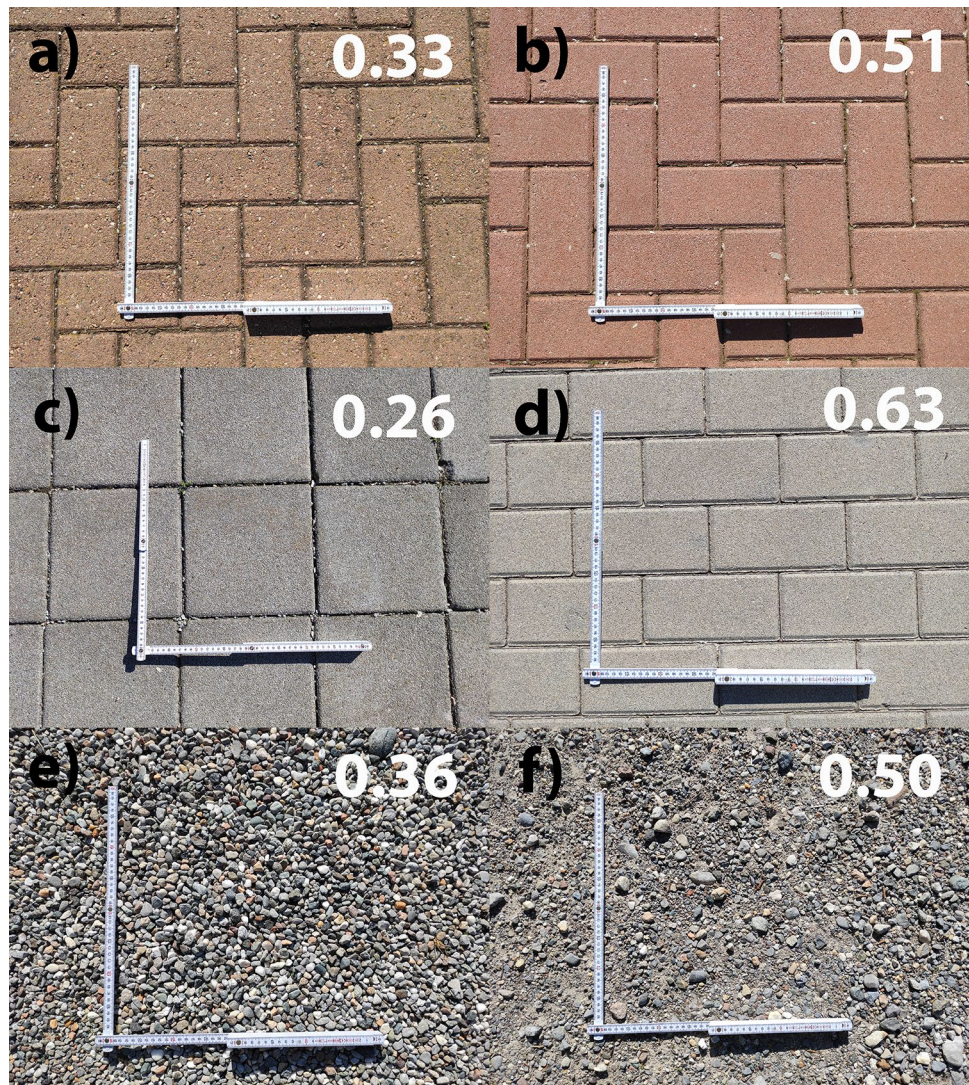
Anthropized surfaces

Generally mitigation strategies on anthropized surfaces focus on the increase of reflectance or the water retention, that is affected by the texture of the material (Santamouris 2013). In this study, anthropized surfaces' ATMIs are mostly amenable by increasing the WC of the material. The surface temperature was only more variable than WC and albedo for porphyry and vibrocompressed concrete, probably due to the increased heat flux exchange through the different type of block inter-connections. This is similar to the different characteristics of seam-fillings (Starke et al. 2011). Surfaces with the lowest WC values like asphalt (33.8%) or pink asphalt (39%) are impervious materials that are the worst choice for the temperature mitigation (Santamouris 2013; Bozdogan Sert et al. 2021). Indeed, not only is such material porosity very low (Nakayama and Fujita 2010), but it is also a homogeneous surface with no interruptions like block grouts that, in the areal complexity, can be more impervious than granite blocks. Therefore, the dimensions of the concrete blocks increase the number of grout as connections with deeper and moister layers (Starke et al. 2011; Qin 2015). We, therefore, suggest that the porosity of the anthropized materials is the only factor responsible for ATMI variability.

Other types of materials displayed low temperature ranges and low ATMI ranges such as asphalts, vibrocompressed concretes 1 and 2, and the holed interlocking pavement. Asphalt is a homogeneous impervious surface, while blocks of vibrocompressed concrete2 showed higher mean temperatures than type 1 and 3 at similar WC because of the reduced presence of grouts (larger dimensions of blocks) that could increase the total surface water retention capacity, namely evaporation (Collins et al. 2010; Starke et al. 2011; Qin 2015). Conversely, the higher permeability of the holed interlocking pavement resulted in low WC due to its low water retention capacity (Qin 2015) (which results in less evaporation).

By grouping the surface types by materials, we can highlight their variability of ATMI and speculate on the proper management/choice for the air temperature warming mitigation. For concrete, it is important to provide as many varieties of grout as possible by reducing the slab/block dimensions (Fig. 5c,d), and to use light colored or pervious concrete (Takebayashi and Moriyama 2012; Qin 2015). Others demonstrated the utility of using reflective concrete, for example adding white components to the mixture (Levinson and Akbari 2002) or increasing its permeability (Matsuo et al. 2005). For gravel, it is important to include different grain sizes to find an equilibrium between drainage and water retention (Qin 2015). This balance is likely obtained with the addition of a soil matrix or mixed grain sizes (Fig. 5e,f), and by utilizing light-colored rocks. It was observed that the age of pink vibrocompressed concrete (Fig. 5a,b) slightly affects the deterioration of material properties by worsening the surface temperature like with thermochromic coatings (Santamouris 2013). Therefore, a cleaning of the surface should be considered both for maintaining a high albedo and an effective infiltration (Mullaney and Lucke 2014). Regarding vibrocompressed concrete and porphyry blocks, similarly to concrete slabs, it is recommended to use small

Fig. 5 Example of same material with different surface type (dimensions) or management and their ATMIs. **a)** vibro-compressed pink concrete1, **b)** vibrocompressed pink concrete2, **c)** vibrocompressed concrete2, **d)** vibrocompressed concrete3, **e)** medium gravel, **f)** mixed gravel



blocks to guarantee an increase of grout (Collins et al. 2010; Mullaney and Lucke 2014), rather than the change of the material color that would change their albedo. Similarly, among asphalts, pink asphalt seemed to be the best solution; not due to its color (albedo), but rather due to its different porosity that led to different WC.

Overall, asphalt is the worst material for the mitigation (Mullaney and Lucke 2014). However, some improvements of the mitigation characteristics of the asphalt can be guaranteed by a better circulation of water within the asphalt grains (De Bondt and Jansen 2006) or the use of light-colored aggregates (Anak Guntor et al. 2014).

After these considerations, we would suggest the choice of small pavements' units, overlaid to properly selected grain sizes that favor the retention of water, able to percolate from the high number of grouts (Mullaney and Lucke 2014). This is a solution that is accessible in multiple urban contexts.

Costs and benefits

The areal extension of the University campus sectors shows that the Valleggio and Bizzozzero sectors contributed to the highest ATMI. This is due to the large vegetated area extension in Bizzozzero and Valleggio, even though some of these areas have recently been converted to parking areas in Valleggio. Conversely, the absence of consistent vegetated areas in Oriani and the large asphalt area in Ravasi made them the worst University zones for climate change mitigation. This is in line with other authors that found it is extremely important to provide green areas in urban landscapes (Takebayashi and Moriyama 2009; Lee et al. 2010; Kong et al. 2014; Mariani et al. 2016; Yao et al. 2019; Tan et al. 2021), especially if they are numerous, large, or fragmented (Kong et al. 2014; Chen and You 2020). This management also helps the mitigation of air temperatures of surrounding surfaces (Kong et al. 2014).

Few works listed the prices of materials for urban building and green planning, probably because the costs are very susceptible to the local economics, and thus highly variable. Lee et al. (2010) listed some general costs for American surfaces that is quite dated. Also Bretz et al. (1998) listed prices for higher albedo materials despite them being dated and focused on the light additives of roofs (which is not the object of this study). Interestingly, Pomerantz (2018) claimed that there is very little monetary energy savings from high albedo materials. The current literature shows no posing costs or green maintenance costs in Italy that include the benefits of natural and anthropized surfaces in urban areas.

In this research, the overall maintenance costs of the green surfaces account for ca. 69,060–82,250 € per year which is 2.3% of the posing costs of the anthropized surfaces. It is known that green surfaces are the best mitigation choice in every case; however, we found other synthetic surface types with interesting ATMI: concrete1, granite block, pink porphyry small block, vibrocompressed concrete3, and white fine gravel. For example, if we take the average cost of the best mitigating materials (concrete1: 28.9 € m⁻² and vibrocompressed concrete3: 30.1 € m⁻²) and substitute the 3 to 8-mowing lawns with these materials, we would obtain a total cost of 11,986,177 € which is equal to ca. 180–197 years of lawn management. This suggests that it is a cheaper solution of management technique, but it is up to the University to decide the future territory planning. On one hand, certain anthropized material (cool pavements) guarantees no future management, but on the other hand, green management is less expensive but requires maintenance (Takebayashi and Moriyama 2009). Probably, the most reasonable choice would be to use concrete in small blocks and as much white as possible (Lee et al. 2010) to maintain the same cost. These could be used for parking areas, pathways or any trampled surface. The use of lawns would also be suitable for recreative or decorative large areas.

Both for green areas and anthropized surfaces, we propose feasible and common solutions to be spread to any urban context, from which local institutions could sustainably save funds. The reduction of green maintenance with suitable vegetation can decrease the annual costs and the choice of smaller pavement's units does not affect the posing costs much more than the choice of another material type.

Conclusion

In this paper, we underlined that surface materials are present with different management strategies and/or surface types and that their surficial temperature is related to their physical characteristics. Using a simple index of mitigation (ATMI), we found higher values for the lawns, while lower

ATMI values for asphalt and porphyry. Among lawns, the best mitigation properties have been found for 3-mowing lawns, due to the fact that taller vegetation is able to provide more shadows, increase the albedo, and retain more water for evapotranspiration. Among anthropized surfaces, despite a general low ATMI, a considerable intra-material variability was observed due to the WC. Therefore, any solution that provides an increase in water retention capacity needs to be considered. For example, the reduction of dimension of the pavement unit guarantees a higher number of inter-blocks connections that increase the whole surface moisture by connecting to the deeper layers. Despite having a minor influence on ATMI, the increase of albedo provided by light-colored materials can also be important.

Since the annual maintenance cost of green areas is 2.3% of the posing costs of the anthropized surfaces, it is recommended to provide green areas with a reduced annual management to reduce the costs. When this is not possible, an alternative is to use pavements with smaller units and light material that would introduce a more expensive initial cost, but would not require future management.

In any case, the increase of green areas would also mitigate CO₂ emissions that can be directly reduced with a greater photosynthetic surface and indirectly with less mowings, fertilizations or clipping removals. A possibility to extend the photosynthetic surface could be the introduction of evergreen species with high LAI such as autochthonous shrub species or hedges.

Acknowledgements We acknowledge University of Insubria for the research grant and the technical offices for the supporting materials. We also acknowledge Dr. John Bills for the English editing support and Centro Geofisico Prealpino for the climatic data provided.

Author contributions SP conducted the fieldwork, computer analysis, figures and tables together with the manuscript writing, while MG has been the responsible of the rationale and conducted the scientific project, as well as substantially helped in the manuscript presentation.

Funding Open access funding provided by Università degli Studi dell'Insubria within the CRUI-CARE Agreement.

Declarations

Conflict of interest The authors declare that they have no conflict of interest.

Open Access This article is licensed under a Creative Commons Attribution 4.0 International License, which permits use, sharing, adaptation, distribution and reproduction in any medium or format, as long as you give appropriate credit to the original author(s) and the source, provide a link to the Creative Commons licence, and indicate if changes were made. The images or other third party material in this article are included in the article's Creative Commons licence, unless indicated otherwise in a credit line to the material. If material is not included in the article's Creative Commons licence and your intended use is not permitted by statutory regulation or exceeds the permitted use, you will need to obtain permission directly from the copyright holder. To view a copy of this licence, visit <http://creativecommons.org/licenses/by/4.0/>.

References

- Addas A, Goldblatt R, Rubinyi S (2020) Utilizing remotely sensed observations to estimate the urban heat Island effect at a local scale: case study of a University campus. *Land*. <https://doi.org/10.3390/LAND9060191>
- Akbari H, Menon S, Rosenfeld A (2009) Global cooling: increasing world-wide urban albedos to offset CO₂. *Clim Change* 94:275–286. <https://doi.org/10.1007/s10584-008-9515-9>
- AnakGuntor NA, Md Din MF, Ponraj M, Iwao K (2014) Thermal performance of developed coating material as cool pavement material for tropical regions. *J Mater Civ Eng* 26:755–760. [https://doi.org/10.1061/\(asce\)mt.1943-5533.0000859](https://doi.org/10.1061/(asce)mt.1943-5533.0000859)
- Anniballe R, Bonafoni S, Pichierrri M (2014) Spatial and temporal trends of the surface and air heat island over Milan using MODIS data. *Remote Sens Environ* 150:163–171. <https://doi.org/10.1016/j.rse.2014.05.005>
- Arghavani S, Malakooti H, Ali Akbari Bidokhti AA (2020) Numerical assessment of the urban green space scenarios on urban heat island and thermal comfort level in Tehran Metropolis. *J Clean Prod* 261:121183. <https://doi.org/10.1016/j.jclepro.2020.121183>
- Asaeda T, Ca VT (1993) The subsurface transport of heat and moisture and its effect on the environment: a numerical model. *Boundary-Layer Meteorol* 65:159–179. <https://doi.org/10.1007/BF00708822>
- Asaeda T, Ca VT (2000) Characteristics of permeable pavement during hot summer weather and impact on the thermal environment. *Build Environ* 35:363–375. [https://doi.org/10.1016/S0360-1323\(99\)00020-7](https://doi.org/10.1016/S0360-1323(99)00020-7)
- Asaeda T, Ca VT, Wake A (1996) Heat storage of pavement and its effect on the lower atmosphere. *Atmos Environ* 30:413–427. [https://doi.org/10.1016/1352-2310\(94\)00140-5](https://doi.org/10.1016/1352-2310(94)00140-5)
- Battista G, Evangelisti L, Guattari C et al (2020) Urban heat island mitigation strategies: experimental and numerical analysis of a university campus in Rome (Italy). *Sustain* 12:1–18. <https://doi.org/10.3390/su12197971>
- Borbora J, Das AK (2014) Summertime urban heat island study for Guwahati City, India. *Sustain Cities Soc* 11:61–66. <https://doi.org/10.1016/j.scs.2013.12.001>
- BozdoganSert E, Kaya E, Adiguzel F et al (2021) Effect of the surface temperature of surface materials on thermal comfort: a case study of Iskenderun (Hatay, Turkey). *Theor Appl Climatol* 144:103–113. <https://doi.org/10.1007/s00704-021-03524-0>
- Bretz S, Akbari H, Rosenfeld A (1998) Practical issues for using solar-reflective materials to mitigate urban heat islands. *Atmos Environ* 32:95–101. [https://doi.org/10.1016/S1352-2310\(97\)00182-9](https://doi.org/10.1016/S1352-2310(97)00182-9)
- Busato F, Lazzarin RM, Noro M (2014) Three years of study of the Urban Heat Island in Padua: Experimental results. *Sustain Cities Soc* 10:251–258. <https://doi.org/10.1016/j.scs.2013.05.001>
- Cao J, Zhou W, Zheng Z, et al (2021) Within-city spatial and temporal heterogeneity of air temperature and its relationship with land surface temperature. *Landsc Urban Plan* 206:103979. <https://doi.org/10.1016/j.landurbplan.2020.103979>
- Cetin M (2015) Using GIS analysis to assess urban green space in terms of accessibility: case study in Kutahya. *Int J Sustain Dev World Ecol* 22:420–424. <https://doi.org/10.1080/13504509.2015.1061066>
- Cetin M (2020) Climate comfort depending on different altitudes and land use in the urban areas in Kahramanmaraş City. *Air Qual Atmos Heal* 13:991–999. <https://doi.org/10.1007/s11869-020-00858-y>
- Cetin M, Aksoy T, Cabuk SN, et al (2021) Employing remote sensing technique to monitor the influence of newly established universities in creating an urban development process on the respective cities. *Land Use policy* 109:105705. <https://doi.org/10.1016/j.landusepol.2021.105705>
- Chen R, You XY (2020) Reduction of urban heat island and associated greenhouse gas emissions. *Mitig Adapt Strateg Glob Chang* 25:689–711. <https://doi.org/10.1007/s11027-019-09886-1>
- Cheval S, Dumitrescu A (2015) The summer surface urban heat island of Bucharest (Romania) retrieved from MODIS images. *Theor Appl Climatol* 121:631–640. <https://doi.org/10.1007/s00704-014-1250-8>
- Christidis N, Jones GS, Stott PA (2015) Dramatically increasing chance of extremely hot summers since the 2003 European heatwave. *Nat Clim Chang* 5:46–50. <https://doi.org/10.1038/nclimate2468>
- Collins KA, Hunt WF, Hathaway JM (2010) Hydrologic comparison of four types of permeable pavement and standard asphalt in eastern North Carolina. *J Hydrol Eng* 15:512–521. [https://doi.org/10.1061/\(asce\)he.1943-5584.0000139](https://doi.org/10.1061/(asce)he.1943-5584.0000139)
- Cotana F, Rossi F, Filipponi M, et al (2014) Albedo control as an effective strategy to tackle Global Warming: A case study. *Appl Energy* 130:641–647. <https://doi.org/10.1016/j.apenergy.2014.02.065>
- Darrel Jenerette G, Harlan SL, Stefanov WL, Martin CA (2011) Ecosystem services and urban heat riskscape moderation: WatfER, green spaces, and social inequality in Phoenix, USA. *Ecol Appl* 21:2637–2651. <https://doi.org/10.1890/10-1493.1>
- Debbage N, Shepherd JM (2015) The urban heat island effect and city contiguity. *Comput Environ Urban Syst* 54:181–194. <https://doi.org/10.1016/j.compenvurbysys.2015.08.002>
- De Bondt AH, Jansen R (2006) Generation and saving of energy via asphalt pavement surfaces. *Fachbeitrag OIB—de Bond*
- Eklund JA, Zhang H, Viles HA, Curteis T (2013) Using handheld moisture meters on limestone: factors affecting performance and guidelines for best practice. *Int J Archit Herit* 7:207–224
- Feng W, Ding W, Zhen M et al (2022) Cooling effect of urban small green spaces in Qujiang Campus, Xi'an Jiaotong University, China. *Environ Dev Sustain* 24:4278–4298. <https://doi.org/10.1007/s10668-021-01615-6>
- Geng Y, Liu K, Xue B, Fujita T (2013) Creating a “green university” in China: a case of shenyang university. *J Clean Prod* 61:13–19. <https://doi.org/10.1016/j.jclepro.2012.07.013>
- Gratani L, Varone L, Bonito A (2016) Carbon sequestration of four urban parks in Rome. *Urban for Urban Green* 19:184–193. <https://doi.org/10.1016/j.ufug.2016.07.007>
- Gu C, Crane J, Hornberger G, Carrico A (2015) The effects of household management practices on the global warming potential of urban lawns. *J Environ Manage* 151:233–242. <https://doi.org/10.1016/j.jenvman.2015.01.008>
- Hardwick SR, Toumi R, Pfeifer M et al (2015) The relationship between leaf area index and microclimate in tropical forest and oil palm plantation: forest disturbance drives changes in microclimate. *Agric for Meteorol* 201:187–195. <https://doi.org/10.1016/j.agrformet.2014.11.010>
- Isotta FA, Frei C, Weigluni V et al (2014) The climate of daily precipitation in the Alps: development and analysis of a high-resolution grid dataset from pan-Alpine rain-gauge data. *Int J Climatol* 34:1657–1675
- KalayciOnac A, Cetin M, Sevik H et al (2021) Rethinking the campus transportation network in the scope of ecological design principles: case study of Izmir Katip Çelebi University Çiğli Campus. *Environ Sci Pollut Res* 28:50847–50866. <https://doi.org/10.1007/s11356-021-14299-2>
- Kinoshita S, Yoshida A, Okuno N (2012) Evaporation performance analysis for water retentive material based on outdoor heat budget and transport properties. *J Heat Isl Inst Int Vol* 7
- Klok EJ (Lisette), Kluck J (Jeroen) (2018) Reasons to adapt to urban heat (in the Netherlands). *Urban Clim* 23:342–351. <https://doi.org/10.1016/j.uclim.2016.10.005>

- Knutson TR, Ploshay JJ (2016) Detection of anthropogenic influence on a summertime heat stress index. *Clim Change* 138:25–39. <https://doi.org/10.1007/s10584-016-1708-z>
- Kong F, Yin H, James P et al (2014) Effects of spatial pattern of greenspace on urban cooling in a large metropolitan area of eastern China. *Landsc Urban Plan* 128:35–47. <https://doi.org/10.1016/j.landurbplan.2014.04.018>
- Kyriakodis GE, Santamouris M (2018) Using reflective pavements to mitigate urban heat island in warm climates—results from a large scale urban mitigation project. *Urban Clim* 24:326–339. <https://doi.org/10.1016/j.uclim.2017.02.002>
- Lee KW, Craver VO, Kohm S, Chango H (2010) Cool pavements as a sustainable approach to green streets and highways. In: *Green Streets Highw 2010 An Interact Conf State Art How to Achieve Sustain Outcomes - Proc Green Streets Highw 2010 Conf* 389:235–247. [https://doi.org/10.1061/41148\(389\)20](https://doi.org/10.1061/41148(389)20)
- Lee H, Mayer H, Chen L (2016) Contribution of trees and grasslands to the mitigation of human heat stress in a residential district of Freiburg, Southwest Germany. *Landsc Urban Plan* 148:37–50. <https://doi.org/10.1016/j.landurbplan.2015.12.004>
- Levinson R, Akbari H (2002) Solar reflectance of cool paving materials effects of composition and exposure on albedo of concrete. *Cem Concr Res* 32:2001–2002
- Lin TP, Matzarakis A, Hwang RL (2010) Shading effect on long-term outdoor thermal comfort. *Build Environ* 45:213–221. <https://doi.org/10.1016/j.buildenv.2009.06.002>
- Marando F, Salvatori E, Sebastiani A et al (2019) Regulating Ecosystem Services and Green Infrastructure: assessment of Urban Heat Island effect mitigation in the municipality of Rome, Italy. *Ecol Modell* 392:92–102. <https://doi.org/10.1016/j.ecolmodel.2018.11.011>
- Marcel C, Villot J (2021) Urban Heat Island index based on a simplified micro scale model. *Urban Clim*. <https://doi.org/10.1016/j.uclim.2021.100922>
- Mariani L, Parisi SG, Cola G et al (2016) Climatological analysis of the mitigating effect of vegetation on the urban heat island of Milan, Italy. *Sci Total Environ* 569–570:762–773. <https://doi.org/10.1016/j.scitotenv.2016.06.111>
- Masson-Delmotte V, Zhai P, Pörtner H-O, et al (2018) Global warming of 1.5 C. An IPCC Spec Rep impacts *Glob Warm* 1
- Matsuo Y, Morino K, Iwatsuki E (2005) A study of porous concrete using electric arc furnace oxidizing slag aggregate. *Bull Aichi Inst Technol Part B* 40:167–217
- Miao SG, Chen F (2014) Enhanced modeling of latent heat flux from urban surfaces in the Noah/single-layer urban canopy coupled model. *Sci China Earth Sci* 57:2408–2416. <https://doi.org/10.1007/s11430-014-4829-0>
- Mirzaei PA, Haghghat F (2010) Approaches to study urban heat island—abilities and limitations. *Build Environ* 45:2192–2201. <https://doi.org/10.1016/j.buildenv.2010.04.001>
- Mirzaei M, Verrelst J, Arbabi M et al (2020) Urban heat island monitoring and impacts on citizen's general health status in Isfahan metropolis: a remote sensing and field survey approach. *Remote Sens* 12:1–17. <https://doi.org/10.3390/RS12081350>
- Morakinyo TE, Ouyang W, Lau KKL et al (2020) Right tree, right place (urban canyon): Tree species selection approach for optimum urban heat mitigation—development and evaluation. *Sci Total Environ* 719:137461. <https://doi.org/10.1016/j.scitotenv.2020.137461>
- Morini E, Touchaei AG, Rossi F et al (2018) Evaluation of albedo enhancement to mitigate impacts of urban heat island in Rome (Italy) using WRF meteorological model. *Urban Clim* 24:551–566. <https://doi.org/10.1016/j.uclim.2017.08.001>
- Mullaney J, Lucke T (2014) Practical review of pervious pavement designs. *Clean: Soil, Air, Water* 42:111–124. <https://doi.org/10.1002/clen.201300118>
- Nakayama T, Fujita T (2010) Cooling effect of water-holding pavements made of new materials on water and heat budgets in urban areas. *Landsc Urban Plan* 96:57–67
- Park J, Kim JH, Sohn W, Li MH (2022) Cooling ranges for urban heat mitigation: continuous cooling effects along the edges of small greenspaces. *Landsc Ecol Eng* 18:31–43. <https://doi.org/10.1007/s11355-021-00481-8>
- Peña MA (2008) Relationships between remotely sensed surface parameters associated with the urban heat sink formation in Santiago, Chile. *Int J Remote Sens* 29:4385–4404. <https://doi.org/10.1080/01431160801908137>
- Picot X (2004) Thermal comfort in urban spaces: impact of vegetation growth: Case study: Piazza della Scienza, Milan, Italy. *Energy Build* 36:329–334. <https://doi.org/10.1016/j.enbuild.2004.01.044>
- Pinna M (1996) Le variazioni del clima. *Fr Angeli* 96
- Pomerantz M (2018) Are cooler surfaces a cost-effect mitigation of urban heat islands? *Urban Clim* 24:393–397. <https://doi.org/10.1016/j.uclim.2017.04.009>
- Ponti S, Cannone N, Guglielmin M (2021a) A new simple topo-climatic model to predict surface displacement in paraglacial and periglacial mountains of the European Alps: the importance of ground heating index and floristic components as ecological indicators. *Ecol Indic*. <https://doi.org/10.1016/j.ecolind.2020.106889>
- Ponti S, Pezza M, Guglielmin M (2021b) The development of Antarctic tafoni: Relations between differential weathering rates and spatial distribution of thermal events, salts concentration and mineralogy. *Geomorphology* 373:107475. <https://doi.org/10.1016/j.geomorph.2020.107475>
- Qin Y (2015) A review on the development of cool pavements to mitigate urban heat island effect. *Renew Sustain Energy Rev* 52:445–459. <https://doi.org/10.1016/j.rser.2015.07.177>
- Ragetti MS, Vicedo-Cabrera AM, Schindler C, Rösli M (2017) Exploring the association between heat and mortality in Switzerland between 1995 and 2013. *Environ Res* 158:703–709. <https://doi.org/10.1016/j.envres.2017.07.021>
- Rahman MA, Stratopoulos LMF, Moser-Reischl A et al (2020) Traits of trees for cooling urban heat islands: a meta-analysis. *Build Environ*. <https://doi.org/10.1016/j.buildenv.2019.106606>
- Rainham DGC, Smoyer-Tomic KE (2003) The role of air pollution in the relationship between a heat stress index and human mortality in Toronto. *Environ Res* 93:9–19. [https://doi.org/10.1016/S0013-9351\(03\)00060-4](https://doi.org/10.1016/S0013-9351(03)00060-4)
- Saadatian O, Bin SK, Salleh E (2013) Adaptation of sustainability community indicators for Malaysian campuses as small cities. *Sustain Cities Soc* 6:40–50. <https://doi.org/10.1016/j.scs.2012.08.002>
- Santamouris M (2013) Using cool pavements as a mitigation strategy to fight urban heat island—a review of the actual developments. *Renew Sustain Energy Rev* 26:224–240. <https://doi.org/10.1016/j.rser.2013.05.047>
- Santamouris M (2014) Cooling the cities—a review of reflective and green roof mitigation technologies to fight heat island and improve comfort in urban environments. *Sol Energy* 103:682–703. <https://doi.org/10.1016/j.solener.2012.07.003>
- Schnepfleitner H, Sass O, Fruhmans S et al (2016) A multi-method investigation of temperature, moisture and salt dynamics in tafoni (Tafraoute, Morocco). *Earth Surf Process Landforms* 41:473–485. <https://doi.org/10.1002/esp.3838>
- Sebastiani A, Marando F, Manes F (2021) Mismatch of regulating ecosystem services for sustainable urban planning: PM10 removal and urban heat island effect mitigation in the municipality of Rome (Italy). *Urban for Urban Green* 57:126938. <https://doi.org/10.1016/j.ufug.2020.126938>
- Sen S, Roesler J (2017) Pavement geometry in microscale urban heat islands. In: *2017 Transportation Association of Canada Conference and Exhibition, TAC 2017*

- Shafique M, Azam A, Rafiq M, Luo X (2020) Evaluating the relationship between freight transport, economic prosperity, urbanization, and CO₂ Emissions: evidence from Hong Kong, Singapore, and South Korea. *Sustainability*. <https://doi.org/10.3390/su122410664>
- Shea C, Jamieson B (2011) Some fundamentals of handheld snow surface thermography. *Cryosphere* 5:55–66. <https://doi.org/10.5194/tc-5-55-2011>
- Srivani M, Hokao K (2013) Evaluating the cooling effects of greening for improving the outdoor thermal environment at an institutional campus in the summer. *Build Environ* 66:158–172. <https://doi.org/10.1016/j.buildenv.2013.04.012>
- Starke P, Göbel P, Coldewey WG (2011) Effects on evaporation rates from different water-permeable pavement designs. *Water Sci Technol* 63:2619–2627. <https://doi.org/10.2166/wst.2011.168>
- Sun T, Sun R, Chen L (2020) The trend inconsistency between land surface temperature and near surface air temperature in assessing Urban heat island effects. *Remote Sens*. <https://doi.org/10.3390/RS12081271>
- Suwartha N, Sari RF (2013) Evaluating UI GreenMetric as a tool to support green universities development: assessment of the year 2011 ranking. *J Clean Prod* 61:46–53. <https://doi.org/10.1016/j.jclepro.2013.02.034>
- Takebayashi H, Moriyama M (2009) Study on the urban heat island mitigation effect achieved by converting to grass-covered parking. *Sol Energy* 83:1211–1223. <https://doi.org/10.1016/j.solener.2009.01.019>
- Takebayashi H, Moriyama M (2012) Study on surface heat budget of various pavements for urban heat island mitigation. *Adv Mater Sci Eng*. <https://doi.org/10.1155/2012/523051>
- Taleghani M (2018) The impact of increasing urban surface albedo on outdoor summer thermal comfort within a university campus. *Urban Clim* 24:175–184. <https://doi.org/10.1016/j.uclim.2018.03.001>
- Tan CL, Wong NH, Jusuf SK, Chiam ZQ (2015) Impact of plant evapotranspiration rate and shrub albedo on temperature reduction in the tropical outdoor environment. *Build Environ* 94:206–217. <https://doi.org/10.1016/j.buildenv.2015.08.001>
- Tan JKN, Belcher RN, Tan HTW et al (2021) The urban heat island mitigation potential of vegetation depends on local surface type and shade. *Urban for Urban Green* 62:127128. <https://doi.org/10.1016/j.ufug.2021.127128>
- Thienelt TS, Anderson DE (2021) Estimates of energy partitioning, evapotranspiration, and net ecosystem exchange of CO₂ for an urban lawn and a tallgrass prairie in the Denver metropolitan area under contrasting conditions. *Urban Ecosyst*. <https://doi.org/10.1007/s11252-021-01108-4>
- Townsend-Small A, Czimeczik CI (2010) Carbon sequestration and greenhouse gas emissions in urban turf. *Geophys Res Lett* 37:1–5. <https://doi.org/10.1029/2009GL041675>
- Vaccari FP, Gioli B, Toscano P, Perrone C (2013) Carbon dioxide balance assessment of the city of Florence (Italy), and implications for urban planning. *Landscape Urban Plan* 120:138–146. <https://doi.org/10.1016/j.landurbplan.2013.08.004>
- Vaz Monteiro M, Doick KJ, Handley P, Peace A (2016) The impact of greenspace size on the extent of local nocturnal air temperature cooling in London. *Urban for Urban Green* 16:160–169. <https://doi.org/10.1016/j.ufug.2016.02.008>
- Whan K, Zscheischler J, Orth R et al (2015) Impact of soil moisture on extreme maximum temperatures in Europe. *Weather Clim Extrem* 9:57–67. <https://doi.org/10.1016/j.wace.2015.05.001>
- Wibowo A, MdYusoff M, Hamzah TAAB, Salleh KO (2019) Urban heat signature impact on university campus. *IOP Conf Ser Earth Environ Sci*. <https://doi.org/10.1088/1755-1315/338/1/012027>
- Wong NH, Kardinal Jusuf S, Aung La Win A et al (2007) Environmental study of the impact of greenery in an institutional campus in the tropics. *Build Environ* 42:2949–2970. <https://doi.org/10.1016/j.buildenv.2006.06.004>
- Xi T, Li Q, Mochida A, Meng Q (2012) Study on the outdoor thermal environment and thermal comfort around campus clusters in subtropical urban areas. *Build Environ* 52:162–170. <https://doi.org/10.1016/j.buildenv.2011.11.006>
- Yamagata H, Nasu M, Yoshizawa M et al (2008) Heat island mitigation using water retentive pavement sprinkled with reclaimed wastewater. *Water Sci Technol* 57:763–771
- Yao L, Xu Y, Zhang B (2019) Effect of urban function and landscape structure on the urban heat island phenomenon in Beijing, China. *Landscape Ecol Eng* 15:379–390. <https://doi.org/10.1007/s11355-019-00388-5>
- Zajch A, Gough WA (2021) Seasonal sensitivity to atmospheric and ground surface temperature changes of an open earth-air heat exchanger in Canadian climates. *Geothermics* 89:101914. <https://doi.org/10.1016/j.geothermics.2020.101914>
- Zeiger E, Farquhar GD, Cowan IR (1987) *Stomatal function*. Stanford University Press
- Zeren Cetin I, Sevik H (2020) Investigation of the relationship between bioclimatic comfort and land use by using GIS and RS techniques in Trabzon. *Environ Monit Assess*. <https://doi.org/10.1007/s10661-019-8029-4>
- Zhou W, Wang J, Cadenasso ML (2017) Effects of the spatial configuration of trees on urban heat mitigation: a comparative study. *Remote Sens Environ* 195:1–12. <https://doi.org/10.1016/j.rse.2017.03.043>
- Ziter CD, Pedersen EJ, Kucharik CJ, Turner MG (2019) Scale-dependent interactions between tree canopy cover and impervious surfaces reduce daytime urban heat during summer. *Proc Natl Acad Sci USA* 116:7575–7580. <https://doi.org/10.1073/pnas.1817561116>